Supporting Information

Sacrificially Formed Nitrogen-Rich CEI from DMI Additive Enhances Reaction Kinetics in Sodium-Ion Batteries

Qiaoyan Lin,[a] Xiaofeng Cai,[a] Wei Han,[b] Yixiang Zhang,[a] Li Zhang,[c] Zeren Zhou,[a] and Lishuang Fan[a]

[a]MIIT Key Laboratory of Critical Materials Technology for New Energy Conversion and Storage, School of Chemistry and Chemical Engineering, Harbin Institute of Technology, Harbin 150001, China.

[b]School of Chemistry, Chemical and Materials Engineering, Taizhou University, Taizhou, Jiangsu 225300, China.

[c]Heilongjiang Tobacco Industrial Co., Ltd. Harbin 150001, China.

Experimental Sections

Preparation of Electrolytes

The additive, 1,3-dimethyl-2-imidazolidinone (DMI), was purchased from Tianjin Kemio Chemical Reagent Co., Ltd. The main components of the reference electrolyte are 1 M $NaClO_4$ dissolved in a 1:1 volume ratio of ethylene carbonate (EC) and diethyl carbonate (DEC), and it also contains a 5% volume fraction of fluoroethylene carbonate (FEC). The modified electrolyte is the commercial electrolyte with different volume fractions of DMI solution added. The amount of additive in the electrolyte is controlled at 1 wt%. All the preparation processes were conducted in Ar-filled gloveboxes.

Synthesis of Mn-Prussian Blue Analogues Mn-PBA

Solution A was prepared by dissolving sodium ferrocyanide ($Na_4Fe(CN)_6 \cdot 10H_2O$) in 50 mL of deionized water to achieve a concentration of 0.05 mol L^{-1} using an analytical balance. Solution B contained manganese sulfate ($MnSO_4 \cdot H_2O$) and trisodium citrate (at a 2:1 citrate to Mn^{2+} molar ratio) in 50 mL deionized water, with $MnSO_4$ concentration fixed at 0.05 mol L^{-1}. Solution C consisted of 100 mL of deionized water maintained at 80°C in an oil bath. Solutions A and B were simultaneously added to Solution C via peristaltic pumps at a constant rate. After complete addition, the mixture was stirred continuously at 80°C for 1 h to ensure thorough reaction, followed by 12 h of static aging. The precipitate was isolated by centrifugation, washed three times with deionized water and once with ethanol, then dried under vacuum at 200°C for 12 h to yield Mn-PBA.

Synthesis of FeMn-PBA-0.5

Solution D was formulated by dissolving 0.025 mol $Na_4Fe(CN)_6 \cdot 10H_2O$ and 5 g NaCl in 50 mL deionized water, purged with N_2 at 80°C. Solution E contained 0.025 mol total of $FeSO_4$ and $MnSO_4$ (1:1 molar ratio), 0.025 mol of trisodium citrate, and 0.1 g of ascorbic acid (VC) in 50 mL of deionized water. Solution E was introduced into Solution D at 1 mL min^{-1} via a peristaltic pump. Following the same centrifugation, washing, and vacuum drying protocol as for Mn-PBA, FeMn-PBA-0.5 was obtained.

Electrochemical Measurement

Sodium vanadium phosphate is used as the active material and mixed with conductive carbon black and Polyvinylidene Fluoride (PVDF) in a mass ratio of 7:2:1. An appropriate amount of N-Methyl-2-pyrrolidone (NMP) is added to adjust the

consistency of the slurry, which is then stirred evenly. The slurry is poured onto a clean aluminum foil and coated using a 200 μm coater. The coated sheet is placed in a vacuum drying oven at 60 ℃ for 12 hours. After drying, the sheet is punched into circular electrode sheets with a diameter of 12 mm, and the mass of each sheet is weighed and recorded for future use. All the batteries in the experiment were assembled using CR2032 battery casings. Before use, the positive and negative battery casings, spring pieces, and gaskets were ultrasonically cleaned in an ethanol solution and dried for later use. Then, the cleaned positive and negative battery casings, glass fiber separators, spring pieces, and gaskets were placed in the battery box and transferred into the glove box through three vacuum extractions in the transition chamber. The glass fibers were cut to a diameter of 16 mm, and the sodium sheets to a diameter of 14 mm, and then placed in the glove box.

Materials Characterization

The morphologies of each sample were observed by Scanning Electron Microscope (SEM, Hitachi SU8010). X-ray Photoelectron Spectroscopy (XPS, Thermo Kalpha) was performed to study the surface chemical properties. The Electrochemical Impedance Spectra (EIS) were recorded with an electrochemical workstation (PARSTAT2273). The electrochemical tests were conducted using a NEWARE battery testing station (BTS-610, Shenzhen, China).

Calculations

Quantum Chemistry Calculations

All the theoretical calculations were calculated by the Gaussian package. The highest occupied and lowest unoccupied molecular orbital (HOMO/LUMO) energy of each molecule was calculated on Density Functional Theory (DFT). The geometry optimization was conducted at B3LYP/6-31+g (d) level, and a higher level of B3LYP/6-311++g (d, p) was applied for the single point calculation.

Molecular dynamics (MD) simulations

MD simulations were performed using Gromacs 2019 with an all-atom optimized potential liquid simulation (OPLS-AA) force field.1 force field parameters for electrolyte components were generated using the LigParGen web server.2 Calculate the 1-scaling CM5 charges using the Multwfn program. 3 The PACKMOL program was used to construct the initial simulation boxes with dimensions of 60 × 60 × 60 $Å^3$ and filled with electrolyte components.

Diffusion coefficient of Na^+ (D_{Na^+})

The diffusion coefficient of sodium-ion (D_{Na^+}) can be determined by the Fick's second law equation:

$$D_{Na+} = \frac{4}{\pi\tau}\left(\frac{m_B V_M}{M_B S}\right)^2\left(\frac{\Delta Es}{\Delta E\tau}\right)^2 \quad (1)$$

where τ is rest interval, m_B is the mass of active material, M_B is the molar mass of active material, V_M is the molar volume of $Na_3V_2(PO_4)_3$ (NVP), S is the geometric area of the electrode sheet, ΔE_S and ΔE_τ can be obtained from GITT curves.

The sodium ion mobility number (t_{Na^+})

Electrochemical Impedance Spectroscopy (EIS) testing is performed on the sodium symmetric cell at an amplitude of 10 mV within the frequency range of 10^4 to 10^{-2} Hz. Constant-potential DC polarization testing is conducted on the same cell under conditions of a polarization voltage of 10 mV and a polarization duration of 3 hours. The sodium ion mobility number is calculated for the polarized cell under identical EIS test conditions by substituting relevant test parameters into equations.

$$t_{Na+} = \frac{I_s(\Delta V - I_0 R_0)}{I_0(\Delta V - I_s R_s)} \quad (2)$$

In the formula, ΔV represents the DC polarization voltage (V); I0 is the initial current value (A); Is is the steady-state current value (A); R0 is the initial resistance (Ω); Rs is the steady-state resistance (Ω).

The relative contributions from diffusion and capacitive processes

The following equation quantitatively describes the current response (i) as a function of scan rate (v) in cyclic voltammetry (CV), revealing the mixed kinetic control mechanisms in electrode reactions.

$$i(V) = k_1 v + k_2 v^{1/2} \tag{3}$$

where $k_1 v$ represents surface-controlled processes, $k_2 v^{1/2}$ is governed by a diffusion-controlled Faradaic process.

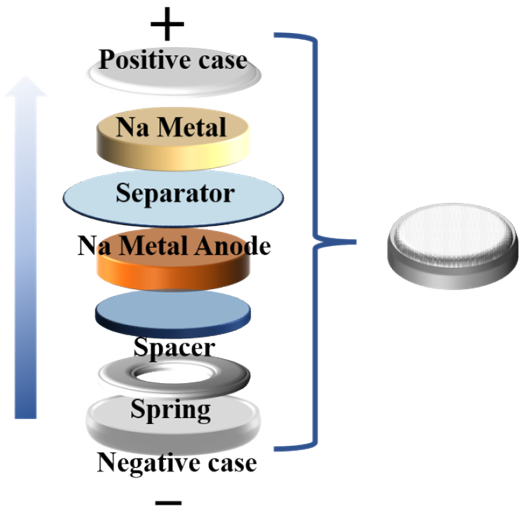

Figure S1. Schematic representation of cell components.

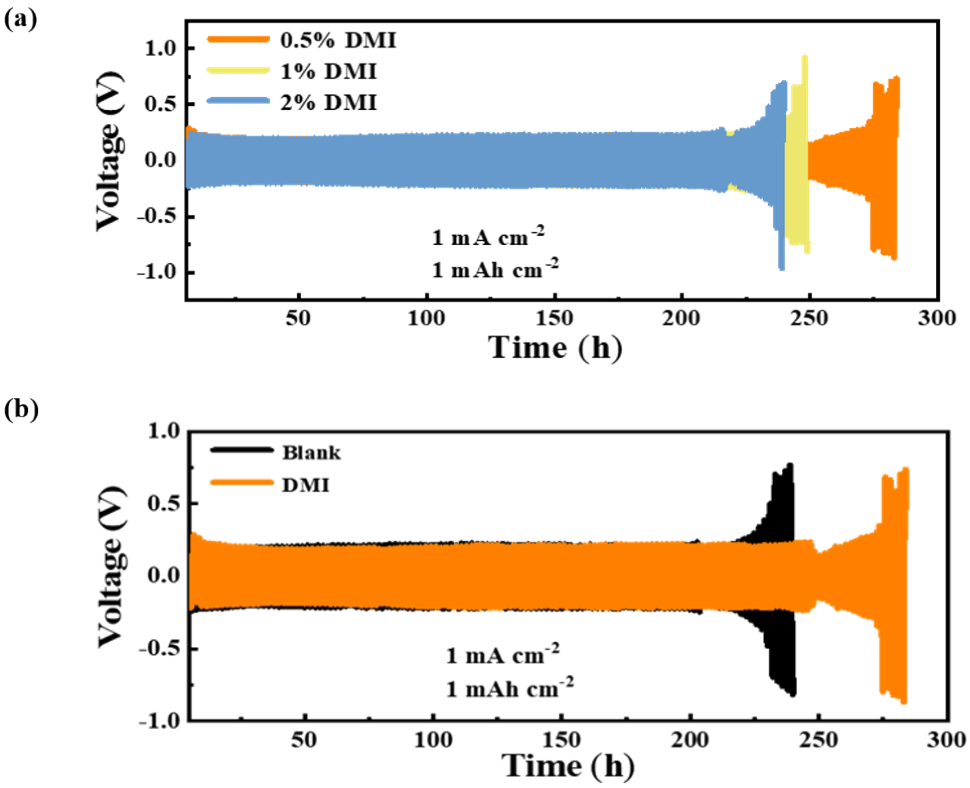

Figure S2. (a) Cycling profiles of baseline and DMI-modified electrolytes, (b) Cycle stability at varying DMI volume fractions.

As shown in Figure S2, the cycling tests were conducted at a current density of 1 mA cm^{-2} with 60 minute plating and stripping cycles per half step.

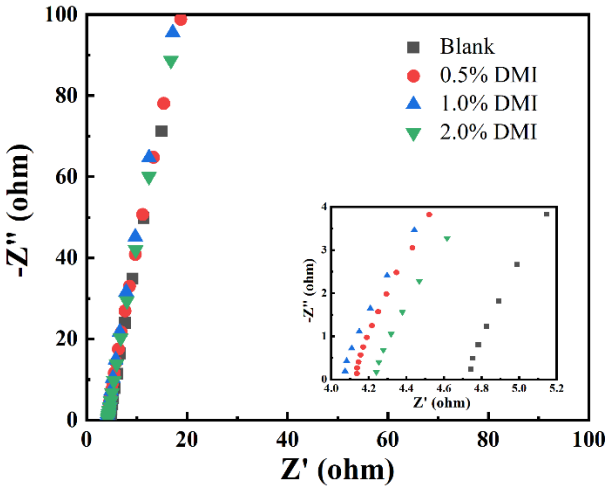

Figure S3. EIS of stainless steel cells across DMI concentrations.

The symmetric cells were assembled using stainless steel blocking electrodes with baseline electrolyte and DMI-modified electrolytes at 0.5%, 1%, and 2% concentrations.

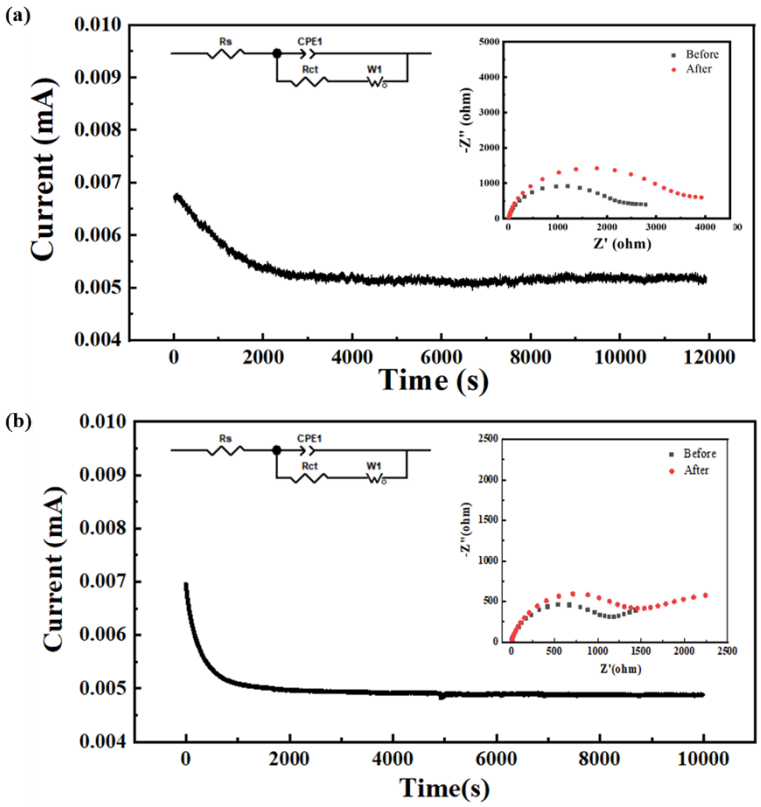

Figure S4. "i-t" curve and EIS of Na||Na symmetric cells: (a) Baseline electrolyte; (b) DMI-modified electrolyte.

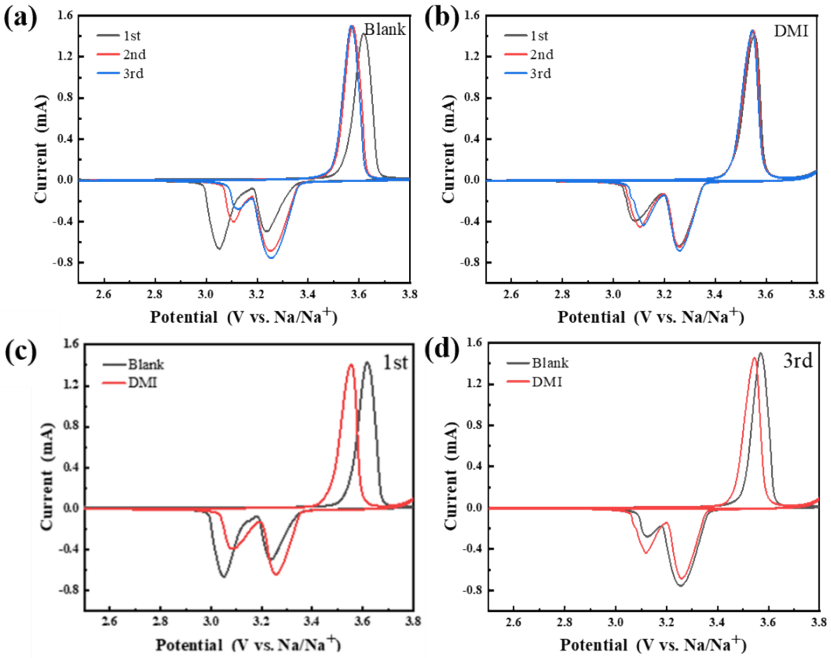

Figure S5. Electrochemical characterization of cells containing baseline and DMI-modified electrolytes:(a) CV curves (baseline), (b) CV curves (DMI-modified), (c) First-cycle voltammograms (comparative), (d) Third-cycle voltammograms (comparative).

The first three cycles of CV tests were conducted at a scanning rate of 0.1 mV s^{-1} within an electrochemical window of 2.5 to 3.8 V.

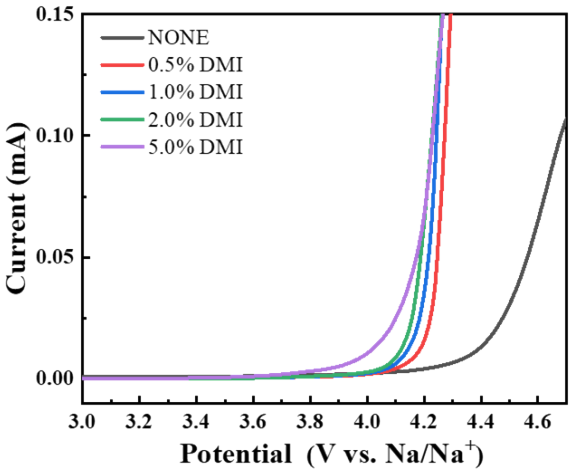

Figure S6. Linear Sweep Voltammetry (LSV) curves at varying DMI volume fractions, Nyquist plots after cycling.

LSV comparisons of baseline electrolyte and DMI-modified electrolytes (0.5-5%) revealed progressively lowered oxidation onset potentials. Oxidation commenced at approximately 4.4 V for the baseline system versus 4.2 V with 0.5% DMI, decreasing to 4.0 V at 5% DMI. This trend originates from DMI's higher HOMO energy level relative to baseline components, inducing preferential oxidation over diethyl carbonate (DEC), which decomposes at approximately 4.4 V. Corroborated by the 3.8 V oxidation peak in cyclic voltammetry, these results demonstrate DMI undergoes oxidative decomposition at the cathode, potentially forming protective polymeric films.

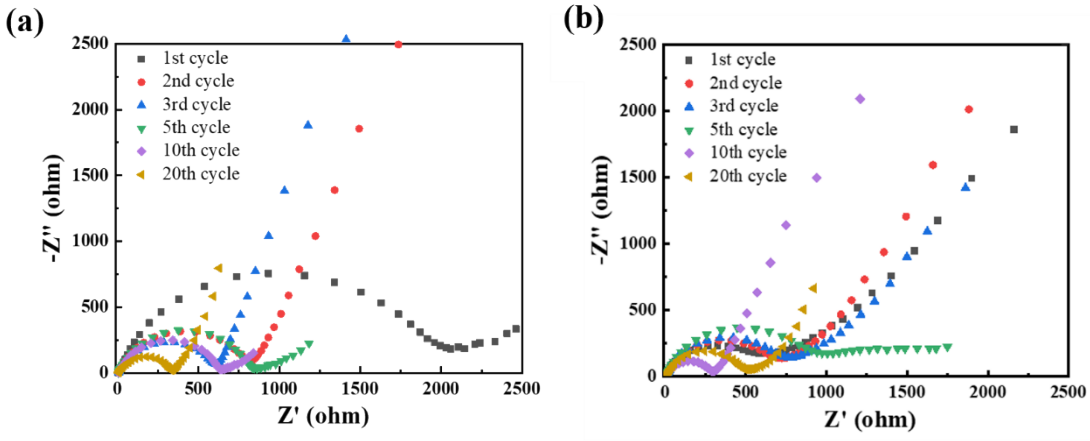

Figure S7. Nyquist plots after cycling: (a) Baseline, (b) DMI-modified.

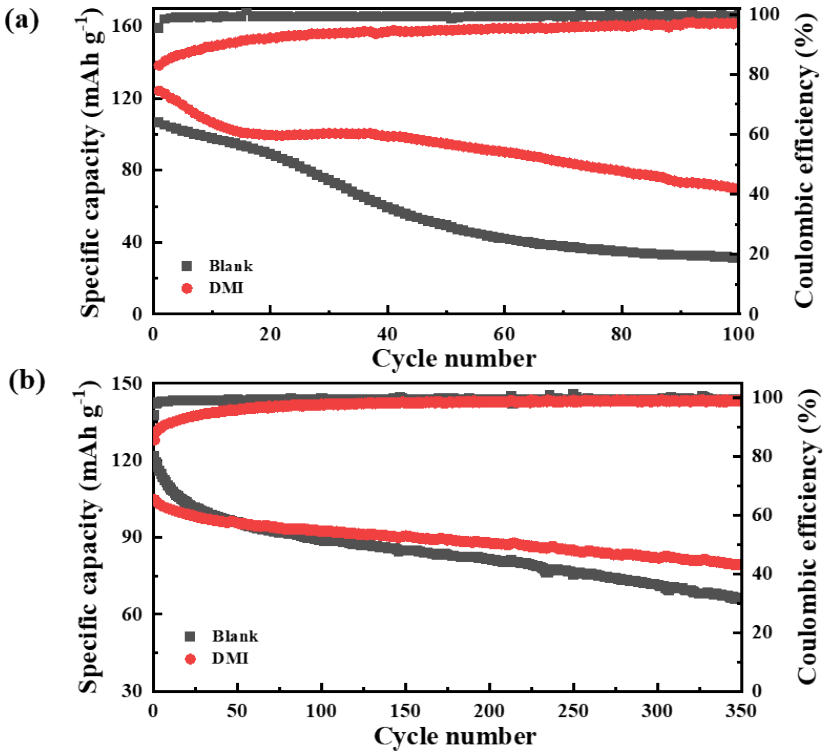

Figure S8. The cyclic voltammograms of (a) Mn-PBA and (b) FeMn-PBA-0.5 materials in the electrolyte system before and after modification.

To evaluate DMI-based electrolytes beyond NVP materials, their effects on Prussian blue analogues (PBAs) were investigated. As shown in Fig S8, half-cells with Mn-PBA and FeMn-PBA-0.5 electrodes were cycled at 1 C, demonstrating that DMI serves as an effective additive. Mn-PBA delivered an initial discharge capacity of 124.2 mAh g^{-1} in the modified electrolyte, with subsequent capacity stabilization outperforming the baseline system, attributed to protective interfacial film formation from DMI decomposition. These results confirm that DMI enhances cathode cycling stability through oxidative decomposition-derived protective films, though inherent PBA limitations (structural vacancies and crystalline water) partially constrain the full benefits.

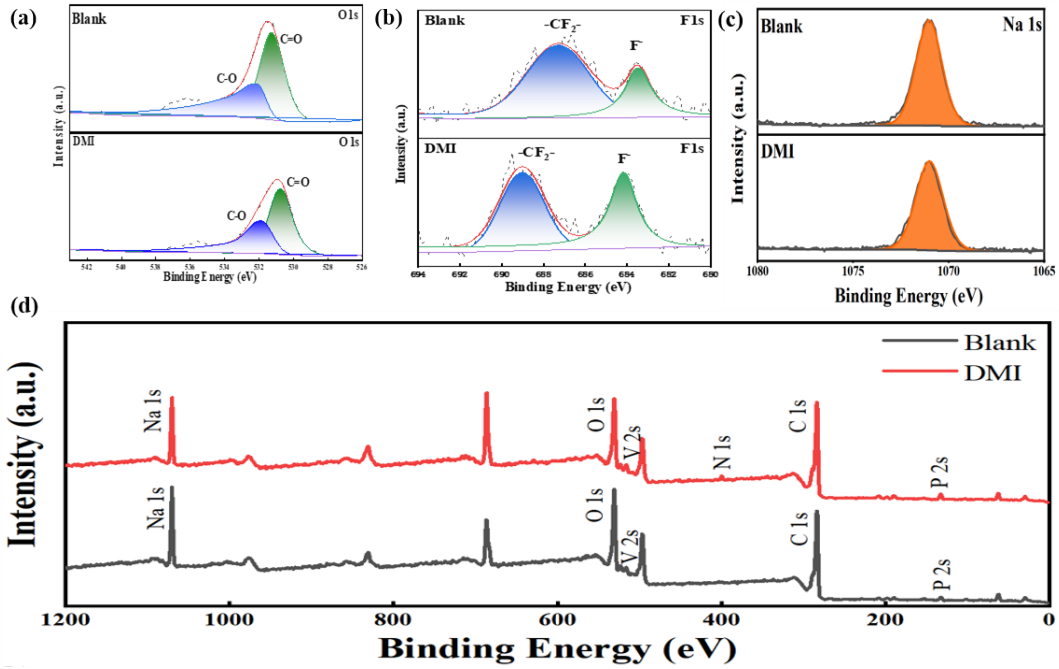

Figure S9. XPS spectra of Solid Electrolyte Interphase **(**SEI) films on cycled anodes in cells with baseline and DMI-modified electrolyte systems: (a) O 1s spectra; (b) F 1s spectra. XPS spectra of Cathode electrolyte interphase (CEI) films on cycled D cathodes:(c) Na 1s spectra; (d) Survey spectra.

Dmi

Additive(s)	**Cathode Material**	**Original Rate Performance**	**Rate after Additive**	**Original Cycling Performance**	**Cycle after Additive**
DMI	NVP	46.9 mAh g^{-1} at 20C	75.3 mAh g^{-1} at 20C	90.2% retention after 200 cycles at 1C; 91.7% retention at 5C after 450 cycles	96.7% retention after 200 cycles at 1C; 94.3% retention after 450 cycles at 5C
EC[1]	NVP	-	-	54.4% retention after 400 cycles at 0.2C	85.3% retention after 100 cycles at 0.2C
1,3,6-Hexanetricarbonitrile (HTCN)[2]	NVP	-	-	80% retention after 300 cycles at 2C	92% retention after 300 cycles at 2C
SbF_3[3]	NVP	79.3 mAh g^{-1} at 20C	72 mAh g^{-1} at 20C	47.1% retention after 400 cycles at 1C	87.2% retention after 400 cycles at 1C
NaFSI[4]	NVP	50.1 mAh g^{-1} at 10C	68.9 mAh g^{-1} at 10C	71.8% retention after 100 cycles at 0.5C	99.3% retention after 100 cycles at 0.5C

Table S1. The magnification and cycle performance before and after adding different types of additives.

References

1. X. Yi, X. Li, J. Zhong, Z. Wang, H. Guo, W. Peng, J. Duan, D. Wang, J. Wang and G. Yan, *Small*, 2023, **19, 2308088**.
2. J. You, Z. Xu, Y. Zhang, Y. Li, B. Zhang, Y. Cao, L. Deng, T. Li and W. Wang, *Chemical Engineering Journal*, 2024, **492, 152198**.
3. W. Fang, H. Jiang, Y. Zheng, H. Zheng, X. Liang, Y. Sun, C. Chen and H. Xiang, *Journal of Power Sources*, 2020, **455, 227956**.
4. L. Li, H. Liu, J. Li, J. Yang, L. Xie, Z. Yi and F. Su, *Chemical Engineering Journal*, 2025, **526, 156-160**.